Reconstruction of Histograms of the Glass Transition Temperature of Free Radical Copolymers from DSC Thermograms

G. FEVOTTE,[1] T. F. MCKENNA[2]

[1] LAGEP-UMR CNRS 5007/ESCPE Lyon, Université Lyon I, 43 Bd du 11 Novembre 1918, 69622 Villeurbanne CEDEX, France

[2] LCPP-CNRS/ESCPE Lyon, Université Lyon I, 43 Bd du 11 Novembre 1918, 69622 Villeurbanne CEDEX, France

Received 11 January 1999; accepted 10 July 1999

ABSTRACT: Most polymeric materials appear as complex mixtures of macromolecules characterized by distributions of specific properties that are essential to the quality of these products. Among such properties, the accurate determination of the glass transition temperature, and therefore, accurate representation of it, is a key issue. When analyzed using dynamic scanning calorimetry (DSC) techniques, many copolymers exhibit a wide range of temperature over which the glass transition takes place, and the width of the transition region is, therefore, not satisfactorily described by average T_g values, for example those computed from tangent curves drawn on thermograms. This article describes a method that allows us to characterize this spreading of the glass transition region by reconstructing weighted T_g distributions from DSC thermograms. As such an objective might appear as questionable from a strictly physical point of view, the significance of what is meant by "distribution" is specified in the text. A model is proposed that accounts for relaxation phenomena. The approach is validated by examining samples of BuA/Sty emulsion copolymers produced at different overall conversions and compositions, and examining the corresponding histograms of T_g were computed. The results show that accurate and consistent information on the glass transition behavior of the copolymer is obtained, and that the effective distribution is clearly connected with the composition drift in the polymer particles. The proposed algorithm allows one to obtain a maximum amount of information from DSC measurements, and provides a deeper insight into the "history" of complex polymer mixtures.
 J Appl Polym Sci 76: 357–367, 2000

Key words: glass transition; differential scanning calorimetry (DSC); copolymer composition; emulsion copolymerization; modeling

INTRODUCTION

The kinetic equations describing monomer consumption during copolymerization processes show that the instantaneous (and overall) copolymer composition is essentially a function of the reactivity ratios and kinetic constants, and the composition of the monomers fed to the reaction loci. In particular, it is well known that composition drifts are often observed during batch or semibatch copolymerization processes unless the reaction takes place at the azeotropic composition (provided that one exists), or if appropriate monomer feed strategies are used.[1] An obvious conse-

Correspondence to: G. Fevotte.

Journal of Applied Polymer Science, Vol. 76, 357–367 (2000)

quence of composition drift is that the distribution of monomer units along the polymer chains is likely to evolve continuously during the copolymerization process, leading to widespread distributions of dyads AA, AB, and BB.

Furthermore, most end-use properties of polymeric materials appear to be so strongly connected to their microstructure that is generally considered that the control of the degree of the evolution of the polymerization process (i.e., conversion, composition of reaction phases) is a prerequisite for the control of the final polymer properties.[1–5] This latter category of variables includes such functions as the molecular weight distribution (MWD), copolymer composition distribution (CCD), and glass transition temperature (T_g). Because the final polymer is a complex mixture of macromolecules, average measurements obtained from final samples can only provide a truncated representation of the "history" and of the distribution of properties such as T_g. Therefore, it is clear that the final distribution of copolymer T_gs—expressed, for example, in terms of histograms—would provide a detailed signature of the entire product process, and consequently, an extremely rich source of information. However, due to the kinetic nature of the glass transition, it is of major importance to explain in the following what we really mean by "T_g distribution."

As far as the control of the polymer properties is concerned, the glass transition temperature of copolymers is one of the more important variables, and many studies have been devoted to the theoretical understanding,[6] to the phenomenological or mechanistic modeling,[7–13] and to the measurement of T_gs in copolymers. As some authors[14] have already noted, knowledge of the average composition and T_g is not sufficient for the characterization of the polymerization product, notably when large composition drifts are expected during the process. By using experimental and simulated data, these authors demonstrated that the same overall chemical composition can result in different T_gs on the one hand, and that a given average value of T_g can be obtained with very different copolymer compositions and microstructures—and, therefore, a wide variety of end uses—on the other hand.

In such a context, common methods used for the determination of T_g from tangent curves drawn on DSC diagrams are rather deceptive. It is the aim of the present article to describe an improved method for the interpretation of DSC thermograms to compute a series of histograms representing the cumulative distribution of the weight fraction of chains in a copolymer exhibiting a rubbery to glassy transition in the same temperature interval. At the expense of a few hypotheses, it is possible to extract histograms of the distribution of T_g that provide a deeper analysis of the copolymer composition and microstructure. As an example, experimental results obtained for the case of the emulsion copolymerization of Styrene (Sty)-*co*-Butyl Acrylate (BuA) are reported here, and the effects of composition drift are clearly demonstrated.

MODELING OF THE DSC THERMOGRAMS

Modeling Objectives

It has been shown that it can be very useful to estimate DSC diagrams from computed composition profiles during batch or semibatch copolymerizations.[14] Such calculations are based on common kinetic and thermodynamic models, and simple equations assuming that the T_g of the copolymer can be assessed at any instant in time from the contribution of dyads produced at that same time.[8,10–12] However, the model-based prediction of DSC thermograms proposed by the authors[14] was not claimed to rigorously fit any experimental data, but rather to provide an efficient tool for the assessment of hypotheses on the physical compatibility of copolymers and, eventually, for the design of "T_g-tailored" polymeric materials. From this latter point of view, a model was proposed in a recent article[15] to predict the time variations of the instantaneous T_gs of STY/BuA emulsion copolymers resulting from possible composition drifts during batch or semicontinuous processes. A nonlinear control law was successfully designed that aimed at tracking any prespecified setpoint T_g profile of the polymeric material through the manipulation of the inlet streams of monomers. Such an approach was presented as a first step towards the on-line control of end-use properties of the copolymers in question. However, to be honest, it should be mentioned that as far as any relationship between the T_g distributions and the end-use properties is not available, the approach mentioned above only remains a slight improvement with respect to "usual" composition control (see, e.g., refs. 1, 16, and 17). As a second step, it is now necessary to validate the model-based predictions of the T_g distri-

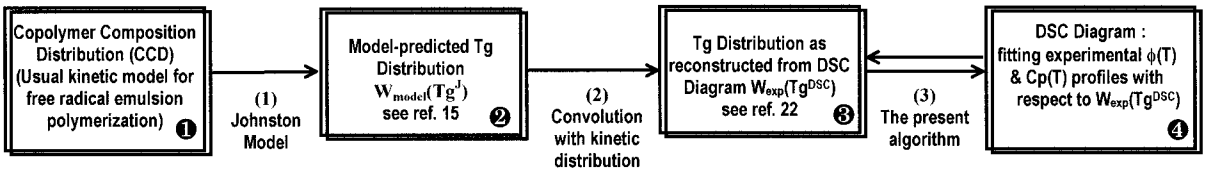

Figure 1 Schematic representation of the various distributions (real and fictitious) considered in the modeling approach.

bution. To do so, DSC was selected to provide *a posteriori* experimental data, and it is the goal of the present article to describe a phenomenological approach that can be used to extract the T_g distribution of samples withdrawn during the polymerization process from DSC thermograms. In the continuity of our work, the logical next step is to design and validate appropriate structure/properties relationships, and then, as a final step, to develop and apply new feedback control strategies for the mastery of specific properties of the polymeric material produced (e.g., mechanical properties).

Actually, when one tries to reproduce experimental data, it becomes apparent that even if the average value of the T_g is rather easy to estimate (see, e.g., refs. 11–12), this is not the case for the distribution of the observed glass transition temperatures (it is not at all evident that this will allow one to explain the relationship between average polymer properties—in particular, the composition—and the width of the temperature interval over which the glass transition is distributed). For example, a comparison between estimated and measured T_gs for various acrylic copolymers was reported in the literature,[18] and significant differences for the same polymer were found; differences that ranged over intervals between 16 and 54°C. According to the author, such discrepancies can be attributed to chemical composition and inaccuracies in homopolymer T_g values reported in the literature. It is also well known that several operating parameters, such as the scanning rate or the thermal history of the sample, can have an effect on the glass transition. In fact, when assessed from DSC measurements, the width of the range of transition temperatures always appears to be larger than that found from the model-based predictions.

In particular, for systems where no composition drift takes place (e.g., copolymers withdrawn from the reactor at very low monomer conversion, or systems at azeotropic composition), the thermal effect of the glass transition is not as stiff as one could expect from constant composition. This fact is obviously attributed to the distribution of the relaxation kinetics involved during the calorimetric scan. In connection with our objective of modeling, the distribution of composition in copolymers in terms of T_g distribution, and even though this might appear as an abuse of the language, we will refer in the following to a "kinetic T_g distribution," associated to any given T_g value. Such kinetic distributions will be denoted by $W_{\exp}(T_g^{\mathrm{DSC}})$, where $W_{f,\exp}(T)$ is the weight fraction of copolymer at which glass transition occurs at temperature T, as explained in more detail below.

In this context, it is not the aim of the present article to draw any conclusions on the enlargement of the glass transition of real copolymers, nor on the variations of the kinetic and thermal effects associated with physical aging. The parameters that are sought to interpret the shape of DSC diagrams do not claim to reveal any physical meaning, but are rather introduced as phenomenological quantities.

Modeling Assumptions

Figure 1 is a schematic representation of the various distributions that will be considered in what follows to extract from DSC thermograms accurate T_g histograms that would be a precise fingerprint of the composition of copolymers. Let us consider a sample of latex withdrawn during the polymerization process. In a rather fictitious way, one can extract a tiny portion of the copolymer characterized by a given individual composition and, consequently, by a T_g value, which, for example, may be evaluated by using the Johnston equation.[11,12,15] The mass of every such "tiny portion" is easy to compute, leading to the distribution $W_{\mathrm{model}}(T_g^{\mathrm{J}})$ mentioned in the second block in Figure 1. During the DSC scanning procedure, it is assumed that any portion of copolymer of given T_g will be subject to the kinetic distribution of the relaxation phenomena. This explains the link number 2 in Figure 1, which can be viewed as a con-

volution leading to the distribution $W_{\exp}(T_g^{\mathrm{DSC}})$ mentioned above.

Another difficulty in the analysis and modeling of DSC experiments arises from the possible phenomena that are generally referred to as physical aging. It is well known that the reversible behavior of polymeric materials near T_g arises from molecular relaxation in the glassy state associated with the tendency of the macromolecules towards a more compact packing. Although it is easy to reduce the phenomena after several temperature scans, a slight thermal effect generally remains at the end of the glass transition front, as a complete quench of the polymer is never fully achieved. A recent article[19] on the viscoelastic behavior of vinylic cellulose copolymers underlines the fact that the application of regression lines for the determination of T_g should take into account the possible relaxation phenomena of the material, because otherwise the T_g values may be different from those of the same material without a relaxation peak. By taking into consideration the overshoots in the DSC diagrams that become more pronounced with physical aging (i.e., link 3 in Fig. 1), it is then assumed that one is in a position to describe the calorimetric measurements in connection with the copolymer distribution of composition.

It what follows, we will consider an increment of temperature (for our purposes an interval of one Kelvin is sufficient) between T and $T + 1$, during which a variation of the copolymer Cp is observed.

Let us now assume that during "very slow" DSC experiments a fictitious "ideal" Cp profile, denoted $Cp^*(T)$ below, would be obtained if no physical aging took place. Obviously, in such a situation, the recorded ideal heat flow $\phi^*(T)$ would not exhibit any overshoot, and the T_g^{DSC} distribution could easily be computed from the corresponding monotonous increment of the heat capacity of the polymer. In reality, the measured heat flow $\phi(T)$ can only be used if one accounts for enthalpy variations due to unpredictable operation-dependent physical aging. Again, it is important to notice that such a statement represents an abuse of the language, because, as outlined by Chartoff,[20] aging endotherms result solely from kinetic effects, and have no latent heat associated with them. Also, it should be mentioned that the physical aging of the polymeric material depends on its composition.

We now assume that $\phi^*(T)$ may be expressed as follows:

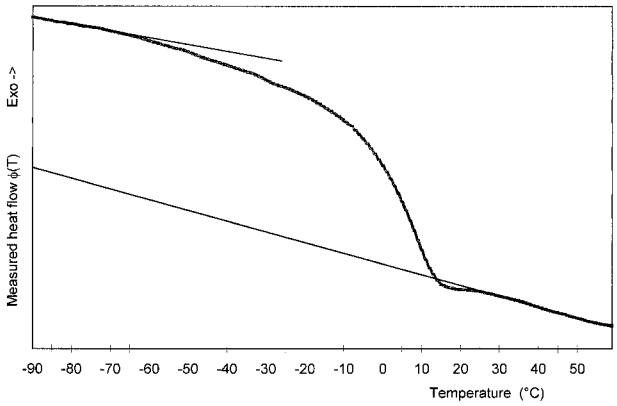

Figure 2 DSC thermogram of a Sty/BuA emulsion copolymer obtained after batch No. 4, with a sample withdrawn after 120 min (cf. Tables I and II). Heating rate: 10 $K \cdot s^{-1}$.

$$\phi^*(T) = m \cdot Cp^*(T) \cdot r \tag{1}$$

where r is the constant heating rate dT/dt in $K \cdot s^{-1}$, $Cp^*(T)$ the instantaneous average "ideal" heat capacity of the polymer sample at temperature T in $J \cdot g^{-1} \cdot K^{-1}$—regardless of its physical state (i.e., full glassy state, partial rubbery state, or full rubbery state), and in the absence of kinetic aspects of the phase transition during heating. m is the mass of sample under consideration in g.

Outside the glass transition region, the reported expressions giving $Cp(T)$ generally take the following form:

$$Cp_{g \text{ or } r}(T) = Cp^{\circ}_{g \text{ or}} + \beta_{g \text{ or } r} \cdot (T - T^{\circ}) \tag{2}$$

where indices g or r refer to polymer at the glassy or rubbery state, respectively, and Cp° is a reference value for the specific heat at temperature T°.

According to Van Krevelen,[13] the curves for the heat capacity of glassy and rubbery polymers may be approximated by straight lines, except below 150 K. Therefore, the four parameters in eq. (2) can be easily estimated from DSC thermograms through the fitting of straight lines measured before and after the glass transition. An example of this is shown in Figure 2 for the case of a Sty/BuA emulsion copolymer exhibiting a significant composition drift. For this experiment, the heating rate was set to 10 $K \cdot s^{-1}$, the mass of sample was 0.0160 g, and two temperature scans were performed before the final record. More details about the experimental part are given below. If a and b

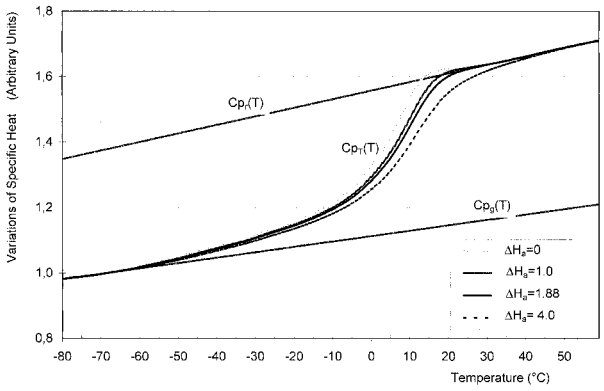

Figure 3 Variations of Cp, as defined by eq. (4), between glassy and rubbery state for different values of the fictitious relaxation enthalpy ΔH_a. The DSC data correspond to Figure 2.

denote the intercept and slope of the recorded portions of thermograms, then one obtains:

$$Cp^{\circ}_{g\ \mathrm{or}} = \frac{a_{g\ \mathrm{or}}}{m \cdot r} \text{ and } \beta_{g\ \mathrm{or}} = \frac{b_{g\ \mathrm{or}}}{m \cdot r} \tag{3}$$

In a given interval $[T, T + dT]$ it is now assumed that the transition from glassy state to rubbery state of a weight fraction of copolymer, dW_g, occurs and that the fictitious parameter $Cp^*(T)$ would be given by the following equation:

$$Cp^*(T) = y_g(T)[Cp^{\circ}_g + \beta_g(T - T^{\circ})] + (1 - y_g(T))[Cp^{\circ}_r + \beta_r(T - T^{\circ})] \tag{4}$$

Where $y_g(T)$ is mass fraction of glassy polymer at temperature T.

The problem now is to relate the fictitious profile $\phi^*(T)$ to the real measured one $\phi(T)$. Given our objective of obtaining suitable information for control purposes, a mechanistic approach appears rather self-defeating, because it would require advanced physical modeling of relaxation kinetics together with the knowledge of a large number of parameters.

By applying eqs. (1) and (4) to the measurements of $\phi(T)$, it is a straightforward exercise to compute the variation of specific heat $Cp(T)$ during the glass transition and, according to the previous hypotheses, the mass m of copolymer at the glassy state as a function of temperature. The result of such computation was obtained from the data in Figure 2, and is displayed in Figures 3 and 4, curve 1. As expected, these results are not consistent, and in particular, due to the relaxation overshoot, negative masses of glassy copolymer are obtained at the end of the glass transition. A simplified phenomenological approach to this problem may lie in the assumption that a part of the measured heat flux $\phi(T)$ is due to the nonequilibrium thermodynamic conditions during the heating process. Taking into account such slight thermal effect would, therefore, allow to reconstruct $\phi^*(T)$ and, consequently, $m(T)$.

However, without any additional assumption, there is an infinity of "black-box" solutions to this problem. For the sake of simplicity, let us assume that some kind of fictitious relaxation enthalpy, denoted ΔH_a below, is associated to the transition of a mass dm of copolymer in the interval $[T, T + dT]$ such that eq. (1) may be rewritten as follows:

$$\phi(T) = m \cdot \left[Cp^*(T) \cdot r + \frac{dy_g(T)}{dt} \cdot \Delta H_a(T) \right] \tag{5}$$

The derivative $(dy_g(T))/dt$ (in s^{-1}) represents the rate of transition to the rubbery state of the sample still containing a mass fraction of glassy polymer y_g, at temperature T.

Even assuming that ΔH_a is constant for the entire range of glass transition temperatures under consideration, the previous assumptions are too broad to allow the calculation of $W_{\mathrm{exp}}(T_g^{\mathrm{DSC}})$ from the measured variation $\phi(T)$, because it is impossible, without additional hypotheses, to distinguish between the effect of the variation of Cp due to partial glass transition and the part of ΔH_a involved.

However, considering that

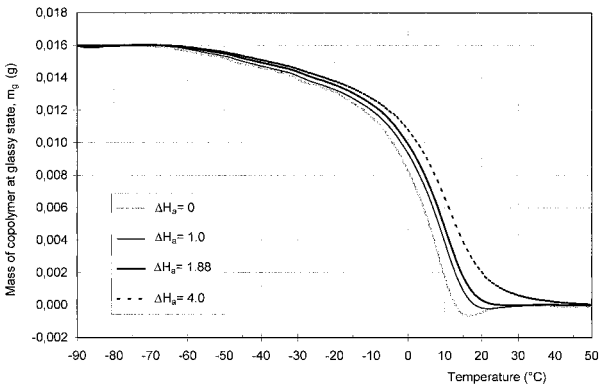

Figure 4 Estimated mass of copolymer at the glassy state against temperature as a function of the fictitious relaxation enthalpy ΔH_a. DSC data in Figure 2.

$$\frac{dy_g(T)}{dT} = \frac{dy_g}{dt}\frac{dt}{dT},$$

eqs. (4) and (5) can be used to compute the decrease of the mass fraction of glassy polymer y_g:

$$\frac{dy_g(T)}{dT} = \frac{\begin{array}{r}\phi(T) - m \cdot r\{y_g(T)[Cp_g^\circ + \beta_g(T - T^\circ)] \\ + [1 - y_g(T)][Cp_r^\circ + \beta_r(T - T^\circ)\}\end{array}}{m \cdot r \cdot \Delta H_a} \tag{6}$$

By using a finite difference approximation, it is now straightforward to calculate the weight fraction W_{exp} of copolymer with T_g^{DSC} belonging to the interval $[T, T + \Delta T]$, and therefore, to reconstruct an histogram of T_gs. In what follows, the width of T_g intervals will be set to $\Delta T = 1$ K:

$$W_g(T) = \Delta y_g(T) \approx \frac{dy_g(T)}{dT}\Delta T \tag{7}$$

It turns out that the derivative dy_g/dT is a function of both the actual value of y_g and ΔH_a and, as mentioned above, the measured $\phi(T)$ does not provide sufficient information to distinguish between physical aging and variation of $Cp^*(T)$. In other words, regardless of the value of ΔH_a, one can always find a solution for $y_g(T)$ that satisfies eq. (6). For example, such solution may be obtained by using Euler's approximation:

$$\begin{aligned}\frac{dy_g(T)}{dT} &\approx \frac{y_g(T) - y_g(T - \Delta T)}{\Delta T} \Rightarrow y_g(T) \\ &\approx \frac{\begin{array}{r}\phi(T)\Delta T + m \cdot r[y_g(T - \Delta T)\Delta H_a \\ - (Cp_r^\circ + \beta_r(T - T^\circ))\Delta T]\end{array}}{\begin{array}{r}m \cdot r \cdot [\Delta H_a + (Cp_g^\circ - Cp_r^\circ \\ + (\beta_g - \beta_r)(T - T^\circ)\Delta T]\end{array}}\end{aligned} \tag{8}$$

With initial condition $y_g(T_{\text{initial}}) = 1$ (e.g., for the DSC thermogram displayed in Fig. 2), the initial condition for the recursive eq. (8) is given by $y_g(-90) = 1$).

As an example, Figure 3 shows several trajectories of $Cp(T)$ computed by using eqs. (5) and (8). The parameters $Cp_{g,r}^\circ$ and $\beta_{g,r}$ were obtained from the linear fitting shown in Figure 2. The variations of the mass of copolymer in the glassy state, $m_g(T) = m \cdot y_g(T)$, which corresponds to the estimates of Cp in Figure 3, are also represented in Figure 4. To illustrate the effect of ΔH_a on the computed Cp profile, these variables were calculated with four different values of ΔH_a between 0 and 4 J/g.

Optimization Strategy

To determine which of the possible values of ΔH_a is appropriate, it is necessary to make an additional assumption. As outlined previously, any underestimation of ΔH_a leads to unrealistic values of the weight fraction of polymer at the glassy state. In particular, the mass of copolymer remaining at the glassy state at the end of the glass transition falls below zero with $\Delta H_a = 0$ or 1 J/g. At the same time, it also appears in Figure 3 that large values of ΔH_a are associated with excessively dispersed estimates of $Cp^*(T)$. Consequently, a critical value ΔH_a^c may be found such that any $\Delta H_a \geq \Delta H_a^c$ leads to acceptable curves for both $m_g(T)$ and $Cp_T(T)$. In this case, however, increasing the enthalpy entails a progressive spreading of the estimated transition temperature range (see, e.g., the estimates obtained with $\Delta H_a = 4$ J/g in Figs. 3 and 4). The measurement of such a dispersion may be calculated as the difference between $Cp^*(T)$ and $Cp_r(T)$, the specific heat at full rubbery state, and it is reasonable to expect that the best estimation of the histograms of T_gs is given by a tradeoff between the computation of negative mass and excessive drift of the glass transition. A mathematical formulation to this problem lies in the search of an optimal combined criteria taking into account these two opposite requirements. For this purpose, the following quadratic criterion may be computed:

$$\begin{aligned}J(\Delta H_a) = \sum_{T=T_g^*}^{T_{\max}} \{\gamma \cdot [Cp_r(T) - Cp^*(T, \Delta H_a)]^2 \\ + \text{Min}\{0, m_g(T, \Delta H_a)\}^2\} = \sum_{T=T_g^*}^{T_{\max}} \{\gamma \cdot \varepsilon_1(T, \Delta H_a)^2 \\ + \varepsilon_2(T, \Delta H_a)^2\}\end{aligned} \tag{9}$$

where $\text{Min}\{0, m_g\}$ denotes the minimal value between 0 and m_g; $T_{\max}$ is the maximal recorded temperature in the considered DSC thermogram; and T_g^* is the temperature where the histogram of T_g presents a maximum, as shown in Figure 5.

In eq. (9), the minimization of criterion ε_2 leads to penalizing possible values of ΔH_a allowing negative transient m_g estimates, and the simultaneous minimization of ε_1 is introduced to reduce, as much as possible, the distance between the

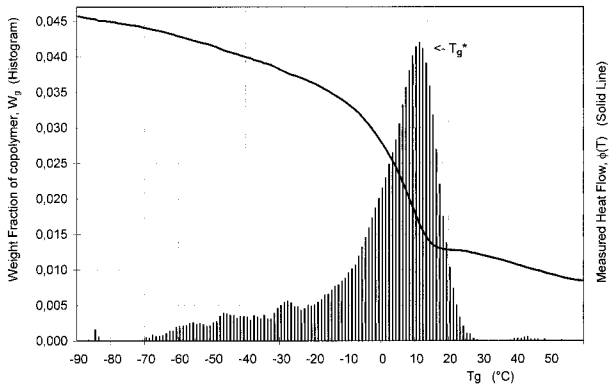

Figure 5 Histogram of the T_g distribution of the copolymer in Figure 2, obtained with the "optimal" relaxation enthalpy $\Delta H_a = 1.88$ J/g.

estimates of Cp^* at the end of the glass transition and Cp_r at full rubbery state defined by eq. (2). To illustrate this twofold objective, the values of ε_1 and ε_2 for $\Delta H_a = 0$ and 4 J/g at $T = 20$°C (i.e., above $T_g^* = 11$°C, in this case) are the following:

$$\varepsilon_1(20,0) = 1.610–1.622 = -0.012;\ \varepsilon_2(20,0) = -4.76\ 10^{-4},\ \text{and}\ \varepsilon_1(20,4) = 0.061;\ \varepsilon_2(20,4) = 0.$$

For this particular data set, the first criterion appears to be in favour of the choice $\Delta H_a = 0$, while the second criterion would lead to select $\Delta H_a = 4$. However, the relative weight of the two criteria is not comparable, because we deal with variables of different physical meaning. To equilibrate the respective effect of the two criteria, the weight factor γ should be tuned carefully. In the following, γ was set to 5.10^5 J · kg^2 · K^{-1}. Actually, the minimization with respect to ΔH_a of the whole "cost function" J, given by eq. (9), leads to the following optimal experimental aging enthalpy:

$$\Delta H_a^{\text{opt}} = \text{Arg}[\underset{\Delta H_a}{\text{Min}}(J(T, \Delta H_a))] \qquad (10)$$

The solution of eq. (10) was searched by using a constrained nonlinear optimization procedure available in the Matlab® Optimization Toolbox.[22] In the case of the DSC thermogram analyzed above, it was found that $\Delta H_a^{\text{opt}} = 1.88$ J/g. The estimates of Cp, m_g, and W_g computed after the optimization of ΔH_a are reproduced in Figures 3, 4, and 5, respectively.

EXPERIMENTAL RESULTS

"Kinetic" T_g Distribution $W_{\text{exp}}(T_g^{\text{DSC}})$

To study the compositional variation of the glass transition temperature in terms of distribution histograms T_g^c, several batch emulsion copolymerizations of styrene and butyl acrylate were carried out at 60°C with different initial monomer mixtures. The feed policies of the different experiments are summarized in Table I. Monomers of commercial grade from Acros Organic Chemical were used without further purification. Potassium persulfate and sodium dodecyl sulphate of extra pure grade were used as initiator and emulsifier, respectively. Before starting the polymerization process, nitrogen was introduced into the initial heel to remove any residual oxygen. Samples were occasionally withdrawn from the reactor, the times and the quantities of which were noted for use in calculating conversions and closing the mass balance. These samples were used to determine the overall weight conversion by gravimetry and the particle size distribution (PSD) by dynamic light scattering, Molecular Weight Distribution by gel permeation chromatography, glass transition temperature using differential scanning calorimetry, and individual conversions using gas chromatography. The main

Table I Feed Policies for the Batch STY/BuA Emulsion Copolymerization Experiments

Batch No.	Water (g)	Styrene (g)	BuA (g)	SDS (g)	KPS (g)
4	3000.5	226.31	526.17	4.31	4.2
5	3000	375	375.84	4.31	4.29
6	3000.1	637.55	116.23	4.31	4.33
7	4000.3	690.05	309.97	5.77	5.76
8	3000.3	112.1	637.54	4.31	4.33

Table II Sty/BuA Emulsion Copolymerizations: Overall and Partial Conversions, Weight Fraction of Monomers in the Particles, Experimental and Computed T_g Values, and "Optimal" Relaxation Enthalpy

Batch No.	Sampling Time (min)	x_g (%)	x_{Sty} (%)	x_{BuA} (%)	W_{sty}	W_{BuA}	T_g (°C) Experimental	T_g^* (°C) Optimized	T_{g_w} (°C) Optimized	T_{g16} (°C)	T_{g50} (°C)	T_{g84} (°C)	ΔH_a (J/g)
8	15	24.1	63.5	17.1	00.4	00.6	−05.5	−03	−04.7	−12.2	−04.4	01.5	2.55
	30	54.7	95.8	47.5	00.3	00.7	−17.2	−11	−11.1	−22.6	−11.7	00.3	5.50
	45	93.6	100.0	92.5	00.2	00.8	−39.1	−23	−18.2	−33.8	−20.1	−03.6	4.03
	120	99.4	100.0	99.2	00.2	00.9	−39.0	−25	−20.4	−35.5	−22.2	−06.2	5.00
4	15	09.6	15.0	07.3	00.5	00.5	18.1	20	14.7	06.9	17.8	22.6	0.83
	30	23.4	35.6	18.2	00.5	00.5	16.9	19	13.3	04.4	16.3	21.2	0.88
	60	39.8	59.7	31.3	00.5	00.5	12.5	15	07.5	−03.3	11.6	17.1	0.86
	90	56.5	81.5	45.7	00.4	00.6	09.9	13	08.3	00.9	10.4	16.3	1.15
	120	68.8	92.4	58.6	00.4	00.6	08.3	11	04.1	−06.3	06.8	14.1	1.51
	150	78.9	98.4	70.5	00.4	00.6	07.6	02	−04.5	−17.2	−03.1	05.6	2.10
	210	93.1	100.0	90.2	00.3	00.7	08.0	08	−02.6	−22.1	01.0	12.4	2.08
5	30	09.1	10.7	07.5	00.6	00.4	37.9	41	40.4	32.8	39.7	46.5	1.07
	60	19.0	21.7	16.2	00.6	00.4	38.8	41	39.9	34.2	39.9	44.8	1.23
	120	34.9	41.0	28.9	00.6	00.4	36.5	39	37.1	31.0	37.3	41.8	0.90
	150	44.4	51.7	37.1	00.6	00.4	35.9	38	36.3	30.2	36.5	41.0	0.81
	180	52.6	61.2	44.0	00.6	00.4	37.0	39	37.6	31.5	37.8	42.8	0.94
	300	83.6	91.3	75.8	00.5	00.5	32.2	35	33.6	27.2	33.6	38.7	0.77
7	15	12.8	12.2	14.1	00.7	00.3	57.8	61	61.2	54.2	60.2	67.3	1.00
	30	32.8	32.6	33.2	00.7	00.3	59.2	62	60.5	55.0	60.4	64.8	0.85
	60	71.2	71.3	70.9	00.7	00.3	58.0	60	58.7	53.0	58.5	63.1	0.73
	90	89.4	89.5	89.3	00.7	00.3	57.5	60	59.0	53.1	58.8	63.8	0.69
	150	96.3	96.4	96.2	00.7	00.3	54.9	58	58.1	51.5	57.7	64.0	1.07
6	15	15.4	15.2	16.9	00.8	00.2	78.0	80	79.6	73.5	79.5	84.6	0.93
	30	25.8	25.4	28.3	00.8	00.2	80.6	82	81.5	76.1	82.2	89.4	0.55
	45	35.1	34.5	38.6	00.8	00.2	80.3	82	79.7	73.7	80.3	84.7	0.71
	60	42.8	42.3	45.4	00.8	00.2	81.7	83	81.7	75.9	82.2	86.7	0.60
	90	59.4	59.1	61.1	00.8	00.2	81.4	83	82.2	76.9	82.2	86.6	0.56
	120	74.5	74.1	76.7	00.8	00.2	80.6	82	81.9	76.0	81.7	87.4	0.53
	200	99.5	99.4	99.8	00.8	00.2	80.2	82	80.4	74.5	80.9	85.5	0.60

data obtained after these measurements are given in Table II.

The DSC thermograms were obtained by using a TA Instrument MDSC 2920 calibrated with high-purity indium. For the needs of this study, we worked at a temperature range of −150 to 120°C at a constant heating rate of 10 $K \cdot min^{-1}$. Liquid nitrogen was used to cool the sample and as the reference for the desired temperature, and a constant argon flow was purged in the reactor cell. As an example, Figure 6 shows a set of thermograms obtained after the batch copolymerization No. 4, with samples withdrawn from the reactor at different time intervals. To reduce the aging effect, we passed all the samples through two initial scans, after which the thermograms were found to be very reproducible. The samples were also dried at 100°C for 24 h to eliminate the effect of solvents on the T_g of copolymers.

Table II shows the overall and partial monomer conversions, the weight fractions of the two monomers in the polymer particles, and the estimates of T_g computed after optimization. Two optimal T_g values are displayed in Table II: the maximal value T_g^*, as defined in eq. (9) and Figure 5, and a weight-average estimate, T_{g_w} calculated from the whole T_g^{DSC} distribution. To shed some light on the validity of the reported average T_g values can be, $T_{g_{16}}$ and $T_{g_{84}}$ were also computed as the temperatures below which 16 and 84%, respectively, are found at the rubbery state. Such values were chosen with reference to Gaussian distributions to provide a simple measurement of the width of the reconstructed distribution. The midpoint in the glass–rubber transition was assessed from usual construction of regression lines on the DSC thermogram, the corresponding value is referred to as "Experimental T_g" in Table II. To illustrate the results, the time variations of the reconstructed T_g histograms obtained after batch Nos. 4 and 5 are presented in Figures 7 and 8, respectively.

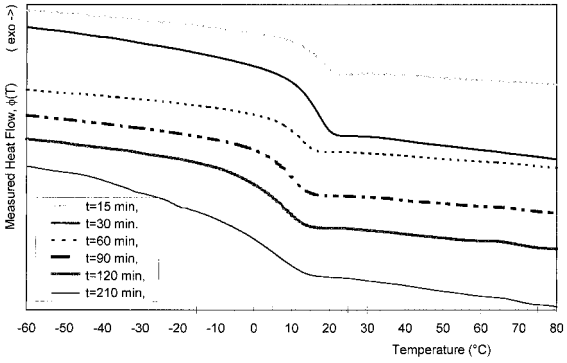

Figure 6 Set of DSC thermograms obtained after batch No. 4.

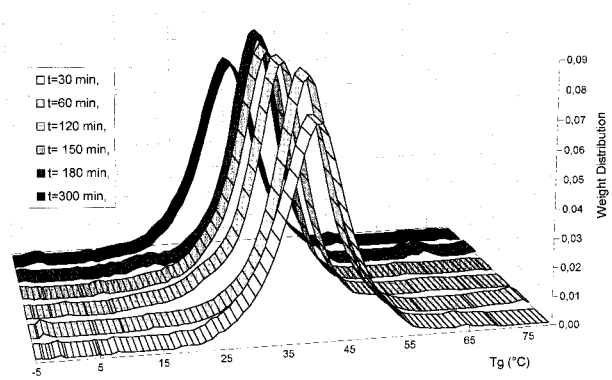

Figure 8 Optimal computed T_g histograms $W_{\text{exp}}(T_g^{\text{DSC}})$ for batch No. 5.

For the copolymer obtained during operation No. 4, a significant drift of the DSC thermograms towards lower temperatures is observed as a function of conversion. This is obviously to be expected because the initial monomer mixture was rich in butyl acrylate, which has a lower glass temperature than styrene. At the beginning of this experiment, the copolymer is composed mainly of styrene which is the more reactive monomer (the reactivity ratios of Sty and BuA are 0.71 and 0.21, respectively). In the case of the fifth experiment, the conversion data in Table II show that only a slight composition drift was obtained during the reaction, and the set of histograms in Figure 8 is, therefore, very consistent. Moreover, Figure 9 represents a comparison between the different computed values of T_g and the "experimental" ones for Experiment 4. The experimental T_g appears to be a good average between the maximum T_g^* and T_{g_w}. However, as outlined by the plots of $T_{g_{16}}$ and $T_{g_{84}}$, even the difference between T_g^* and T_{g_w} is obviously insufficient to give a precise idea of the real distribution, and therefore, of the composition drift. It can also be noted that the seventh operation was performed very closed to the azeotropic composition (69% Sty/31% BuA). In this case, a constant instantaneous copolymer composition was expected. As one can see in Table II, only a slight composition drift has been observed at the beginning of this copolymerization experiment, and both the average T_g estimates and the distributions of histograms remained almost constant.

"Composition" T_g Distribution $W_{\text{model}}(T_g')$

As outlined in Figure 1, the distribution of interest for our control purpose is $W_{\text{model}}(T_g^{\text{J}})$, which is directly connected to the Copolymer Composition Distribution (CCD) through the relationship No. 1. The demonstration of the consistency between $W_{\text{model}}(T_g^{\text{J}})$, $W_{\text{exp}}(T_g^{\text{DSC}})$ and CCD was published in a recent article,[22] and the reported experimental results may be considered as *a posteriori* valida-

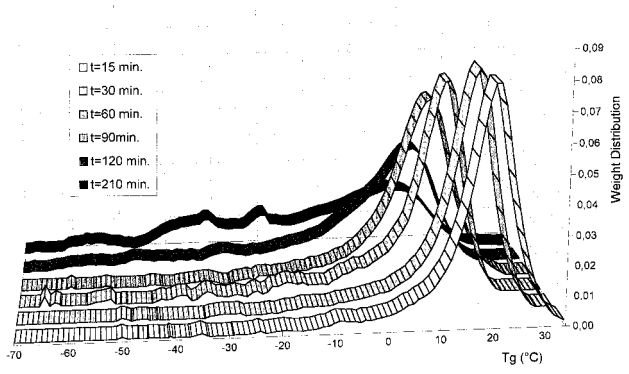

Figure 7 Optimal computed T_g histograms $W_{\text{exp}}(T_g^{\text{DSC}})$ for batch No. 4.

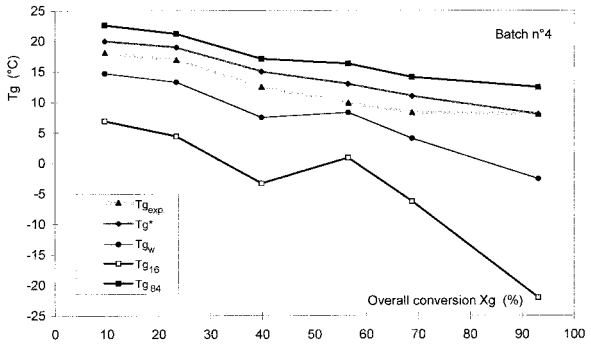

Figure 9 Experimental and computed T_g values as a function of the overall conversion after the batch copolymerization No. 4.

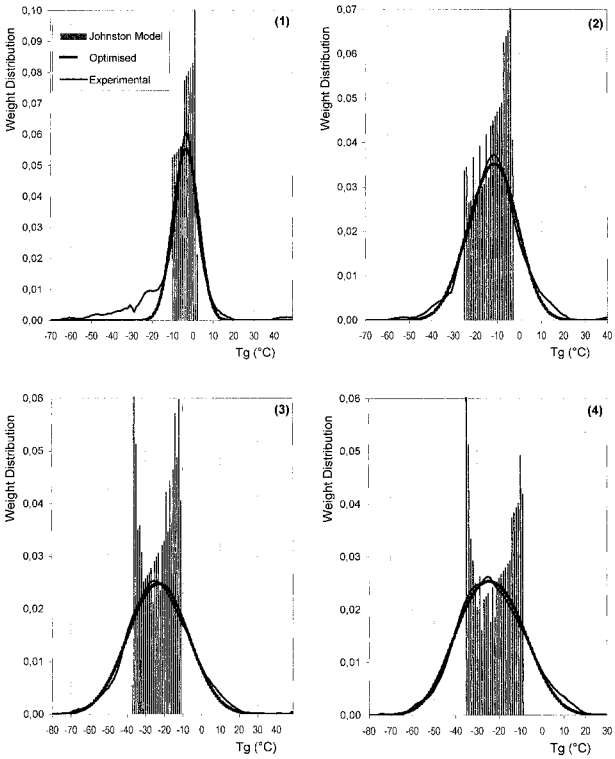

Figure 10 Comparison of the histograms of T_g distribution for the batch copolymerization No. 8. $W_{\text{model}}(T_g^{\text{J}})$ is computed with the Johnston equation (see refs. 15 and 22), $W_{\text{exp}}(T_g^{\text{DSC}})$ is the "experimental" distribution reconstructed from DSC thermograms and the "optimized" result is the T_g^{DSC} distribution predicted from $W_{\text{model}}(T_g^{\text{J}})$, as described in ref. 22. (1) time = 15 min; (2) time = 30 min; (3) time = 45 min; (4) time = 120 min.

tion of the technique presented here. To enlighten the full modeling approach, only two significant results will be recalled now:

1. The $W_{\text{exp}}(T_g^{\text{DSC}})$ distributions can easily be generated with good precision using the CCD predicted from a "classic" free radical copolymerization model.[15] To do this, a two-step procedure can be used: (a) the histograms corresponding to $W_{\text{model}}(T_g^{\text{J}})$ are calculated using the Johnston model. This model requires values of the T_g of the two homopolymers, as well as a T_g that corresponds to that of a perfectly alternating copolymer. This last quantity is generally referred to as T_{g12}. (b) A convolution of the histograms using a Gaussian distribution, the average of which is the same as that of $W_{\text{exp}}(T_g^{\text{DSC}})$, and that has a practically constant standard distribution that does not vary as a function of the composition over the range of values considered here.
2. Results obtained from batch No. 8 are shown in Figure 10 as an example of this operation. The optimization of all of the experiments performed here allowed us to show that the parameter $T_{g_{12}}$ used in the Johnston equation is not constant as originally supposed, but rather varies as a function of the composition. This is shown as a function of the overall fraction of BuA in the copolymer in Figure 11. In addition, it also appears that the values of T_g for the two homopolymers found from the optimization described above are coherent with those presented in the literature. For example, Penzel et al.[23] give a value of 240 K for the T_g of BuA vs. a value of 236 K found here.

CONCLUSION

Commonly used rules for assessing the T_g of polymers from DSC thermograms reflect the ambiguity of reducing the glass-transition range to only one T_g value. In particular, these rules require us to make some arbitrary choice between several possible T_g values obtained after simple plots, and fail to provide any relevant measurement of the width of the transition range. To cope with such difficulties, a method was proposed here with which one can reconstruct the T_g distribution of copolymers in terms of weight histograms from typical DSC thermograms. Simple assumptions were made to account for the effect of phys-

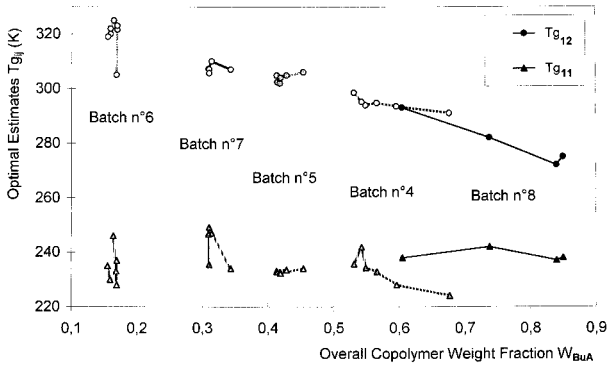

Figure 11 Optimal estimates $T_{g_{11}}$ and $T_{g_{12}}$ for the entire set of copolymer samples with only $T_{g_{22}}$ (pSTY) assumed known.

ical aging and other kinetic aspects during the glass transition of a given polymer sample in the computation of the weight fraction of copolymer characterized by a given T_g interval. To fit the model from the recorded DSC thermograms, a combined quadratic criterion was minimized with respect to some fictitious enthalpy, and assumed to provide the "best" estimate of the T_g distribution.

To validate the approach, samples of BuA/Sty emulsion copolymers were produced with various conversions and composition drifts. An analysis of the results show that an improved estimation of the T_g distribution was obtained, which was clearly connected with the composition drift of the polymer particles. It is reasonable to expect that the proposed optimization procedure can be used to more fully exploit DSC measurements and to obtain a deeper insight into the "history" of complex polymer mixtures.

REFERENCES

1. Canu, S.; Canegallo, S.; Morbidelli, M.; Storti, G. J Appl Polym Sci 1994, 54, 1899.
2. Ray, W. H. Polymer Reaction Engineering; Reichert, K. H.; Geiseler, W., Eds.; VCH Publishers: Wein, 1989.
3. Ponnuswamy, S.; Shah, S.; Kiparissides, C. J Appl Polym Sci 1986, 32, 3239.
4. Dimitratos, J.; Georgakis, C.; El-Aasser, M.; Klein, A. Chem Eng Sci 1991, 46, 3203.
5. Van Doremaele, G. H. J.; Schoonbrood, H. A. S.; Kurja, J.; German, L. J Appl Polym Sci 1992, 45, 945.
6. Gibbs, J. H.; DiMarzio, E. A. J Chem Phys 1958, 28, 373.
7. Fox, T. G.; Loshaek, S. J Polym Sci 1955, 15, 371.
8. Fox, T. G. Bull Am Phys Soc 1956, 1, 123.
9. Couchman, P. R. Polym Eng Sci 1981, 21, 377.
10. Couchman, P. R. Macromolecules 1982, 15, 770.
11. Johnston, N. W. Macromolecules 1973, 6, 453.
12. Johnston, N. W. Polym Preprints 1973, 14, 46.
13. Van Krevelen, D. W. Properties of Polymers, Their Correlation with Chemical Structure, Their Numerical Estimation and Prediction from Additive Group Contributions; Elsevier: Amsterdam, 1990, 3rd ed.
14. Guillot, J.; Emelie, B. Makromol Chem Rapid Commun 1991, 12, 117.
15. Févotte, G.; McKenna, T. F.; Hammouri, H.; Othman, S. Chem Eng Sci 1998, 53, 773.
16. Guillot, J.; Graillat, C. J Makromol Sci Chem 1984, A21, 683.
17. Leiza, J. R.; de la Cal, J. C.; Montes, M.; Asua, J. M. Process Control Quality 1993, 4, 197.
18. Gupta, M. K. J Coating Technol 1995, 67, 53.
19. Flaqué, C.; Montserrat, S. J Appl Polym Sci 1993, 47, 595.
20. Chartoff, R. P. In Thermal Characterization of Polymeric Materials: Turi, E. A., Ed.; Academic Press: New York, 1997, 2nd ed.
21. Grace, A. Optimization Toolbox for Use with Matlab®; The MathWorks Inc.: Natick, MA, 1992.
22. Févotte, G.; McKenna, T. F.; Santos, A. M. Chem Eng Sci 1998, 53, 2241.
23. Penzel, E.; Reiger, J.; Schneider, H. A. Polymer 1997, 38, 325.